Velocity-Vorticity Patterns in Turbulent Flow

Richard B. Pelz, Victor Yakhot, and Steven A. Orszag

Princeton University, Princeton, New Jersey 08544

and

Leonid Shtilman[a] and Evgeny Levich

City College of the City University of New York, New York, New York 10031

Direct numerical simulation of the Navier-Stokes equations is used for the investigation of local helicity fluctuations in plane Poiseuille (channel) and Taylor-Green vortex flows. It is shown that in regions of high dissipation, the cosine of the angle between velocity and vorticity is evenly distributed; in regions of low dissipation, the velocity and vorticity vectors have a tendency to align. It is also shown that near the central part of the channel, velocity and vorticity vectors have a strong tendency to be aligned, while in the buffer region, all angles are nearly equally probable.

The Navier-Stokes equations in rotation form are

$$\frac{\partial \mathbf{u}}{\partial t} - \mathbf{u} \times \boldsymbol{\omega} = -\nabla\left(\frac{P}{\rho} + \frac{1}{2}u^2\right) + \nu \Delta \mathbf{u}, \qquad (1)$$

where the vorticity is $\boldsymbol{\omega} = \nabla \times \mathbf{u}$. It is plausible that regions of large turbulent activity are correlated with regions of large $\mathbf{u} \times \boldsymbol{\omega}$ and, hence, relatively small helicity density $\mathbf{u} \cdot \boldsymbol{\omega}$. It has also been suggested[1-5] that helicity fluctuations may be related to coherent structures and small-scale intermittency in turbulent flows. Some support for this latter conjecture has been given by analysis of geophysical[6-8] and laboratory experimental data.[2] Here we investigate the role of helicity-density fluctuations using direct numerical simulation of turbulent channel flow and the Taylor-Green vortex.

We have used a pseudospectral computer code[9] to solve the Navier-Stokes equations. For channel flow, periodic boundary conditions are assumed in the streamwise (x) and spanwise (y) directions, and the no-slip condition is imposed at the walls. Typical runs use 32 Fourier modes in the streamwise and spanwise directions and 33 Chebyshev modes in the normal (z) direction. The channel dimensions are $2\pi\delta$ (x), $\pi\delta$ (y), and 2δ (z) where δ is the channel half-width. The Reynolds number is 194 based on the wall shear velocity, channel half-width, and kinematic (molecular) viscosity. The turbulence evolves significantly on a nondimensional time of 10. The code is run long enough ($t \approx 60$) for a nearly stationary-state turbulent flow to develop. No subgrid turbulence model is used since the grid gives adequate resolution of all energy-containing scales. The Taylor-Green vortex (at $N_{Re} = 1500$) is computed using a very special and efficient code based on symmetries in the Taylor-Green initial conditions.[10]

In Fig. 1(a), we plot the non-normalized probability density $P(\cos\theta)$ where $\cos\theta = \mathbf{u} \cdot \boldsymbol{\omega}/(|\mathbf{u}||\boldsymbol{\omega}|)$ for channel flow. All information plotted is from a single realization and a single time. No averaging is done; however, all samples tested gave the same mean result. An unexpected and somewhat striking feature of the distribution is the appearance of two peaks corresponding to $|\cos\theta| = 0$ and $|\cos\theta| = 1$. The $\cos\theta = 0$ peak can be explained by the existence of the (quasilaminar) viscous sublayer close to the wall where $\mathbf{u} \cdot \boldsymbol{\omega} = 0$. Indeed, the same probability-density function measured in the center region of the channel ($z_+ = zu_\tau/\nu > 15$) [see Fig. 1(b)] does not show the maximum at $\cos\theta = 0$ while the sharp peak at $|\cos\theta| = 1$ persists. When the distribution function is evaluated by excluding both the wall and central part of the channel ($15 < z_+ < 40$), the probability density $P(\cos\theta)$ [see Fig. 1(c)] is much flatter.

We conclude that, while the vorticity is mainly in the spanwise direction near the rigid wall, towards the center of the channel, the large-scale vorticity is being convected by and aligned with the mean flow. The large-scale turbulent features away from the walls are approximately force-free or Beltrami-like in character in that $\mathbf{u} \times \boldsymbol{\omega}$ is relatively small. This characterization of flow structures away from the walls as approximately force-free flows may be useful in developing models of coherent eddies in turbulent flows. Indeed, recent studies[11] of free shear flows show similar behavior of large-scale flow features.

The role of helicity-density fluctuations is clarified by analyzing the probability distribution $P(\cos\theta')$, where $\cos\theta' = \mathbf{u}' \cdot \boldsymbol{\omega}'/(|\mathbf{u}'||\boldsymbol{\omega}'|)$, $\mathbf{u}' = \mathbf{u} - \langle \mathbf{u} \rangle$ and $\boldsymbol{\omega}' = \nabla \times \mathbf{u}'$ are the fluctuating velocity and vorticity components and $\langle \; \rangle$ indicates horizontal average. As shown by the results plotted in Fig. 2(a), the distribution of $\cos\theta'$ over the full channel is much flatter than the $\cos\theta$ distribution plotted in Fig. 1(a). However, in the region $15 < z_+ < 40$, the distributions of $\cos\theta$ and
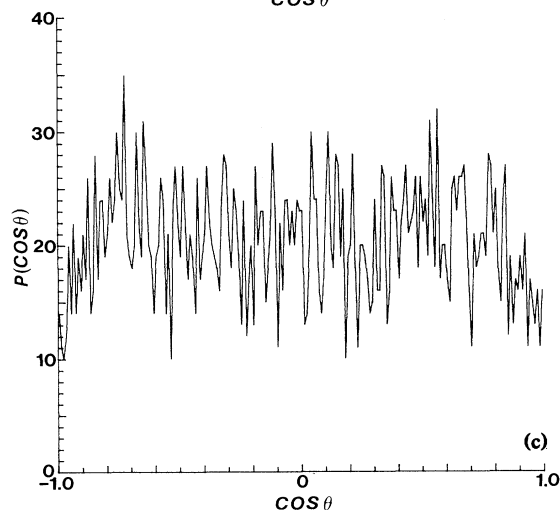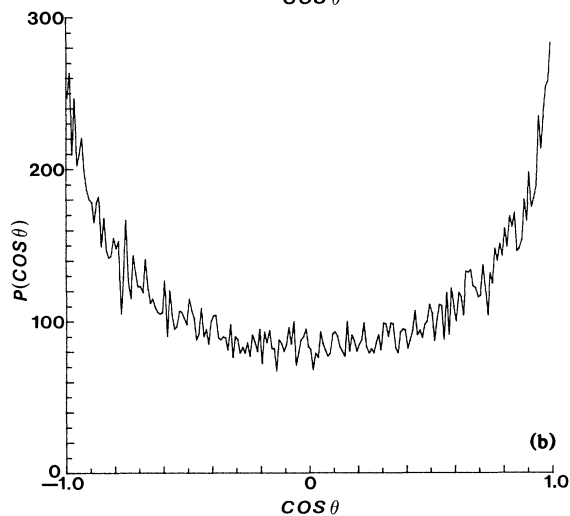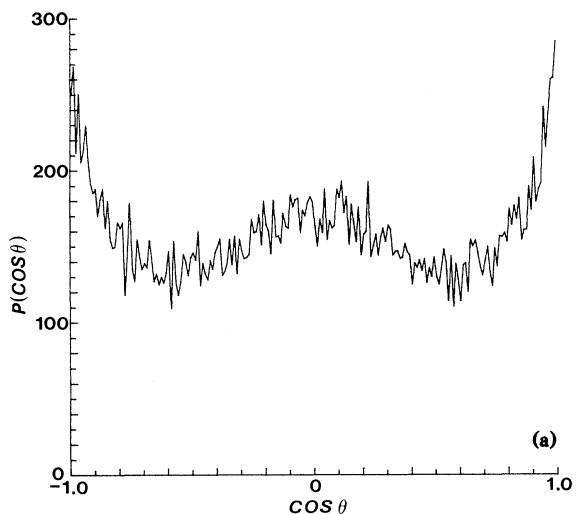
FIG. 1. The probability density for the distribution of the angle between velocity and vorticity in channel flow: (a) throughout the channel; (b) in the center part of the channel ($z_+ > 15$); (c) in the buffer region of the channel ($15 < z_+ < 40$).
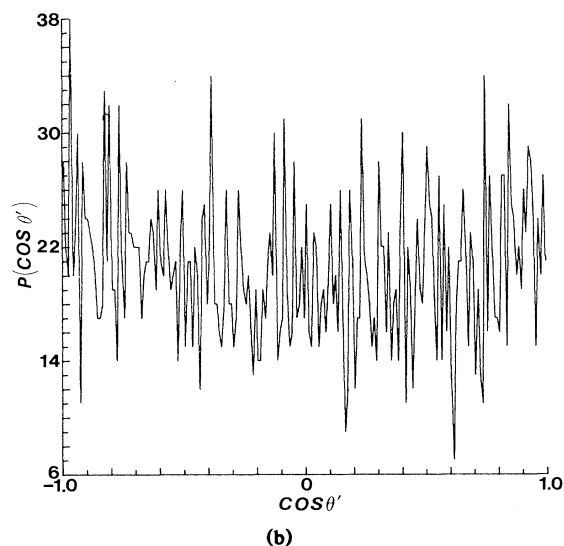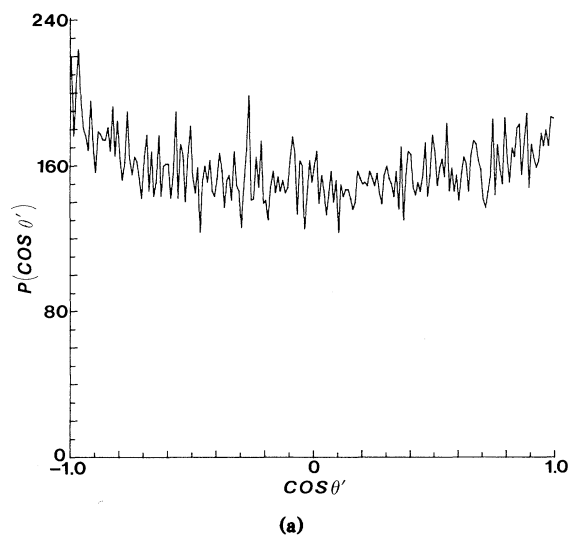

FIG. 2. The probability density for the distribution of the angle between fluctuating velocity $\mathbf{u}'$ and vorticity $\boldsymbol{\omega}'$: (a) throughout the channel; (b) in the buffer region of the channel ($15 < z_+ < 40$).

$\cos\theta'$ are similar [cf. Figs. 2(b) and 1(c)]. We conclude that the sharp peak at $|\cos\theta| = 1$ seen in Figs. 1(a) and 1(b) is related to properties of the large-scale flow.

Results from conditional sampling in regions where the dissipation, $S_{ij}^2 = \frac{1}{2}(\partial u_i/\partial x_j + \partial u_j/\partial x_i)^2$, is large and small yield drastically different probability distributions. In Figs. 3(a) and 3(b) we plot probability densities for the channel and Taylor-Green problems, respectively. In sampled regions where $S_{ij}^2 > 0.3 \times \max S_{ij}^2$, the distribution is nearly uniform. In regions where $S_{ij}^2 < 0.05 \max S_{ij}^2$ [Figs. 4(a) and 4(b)] there is a high probability that the velocity and vortici-
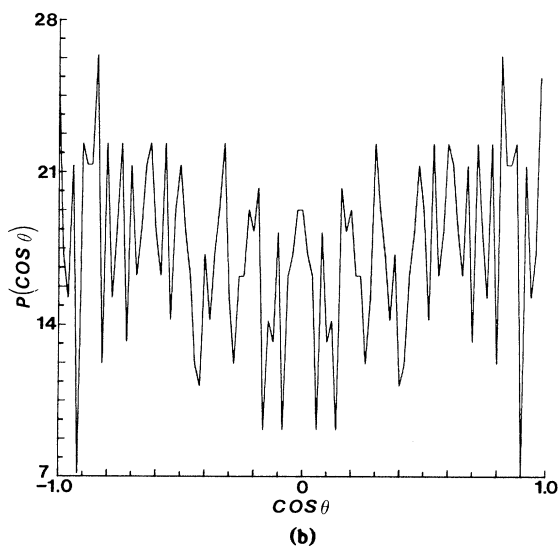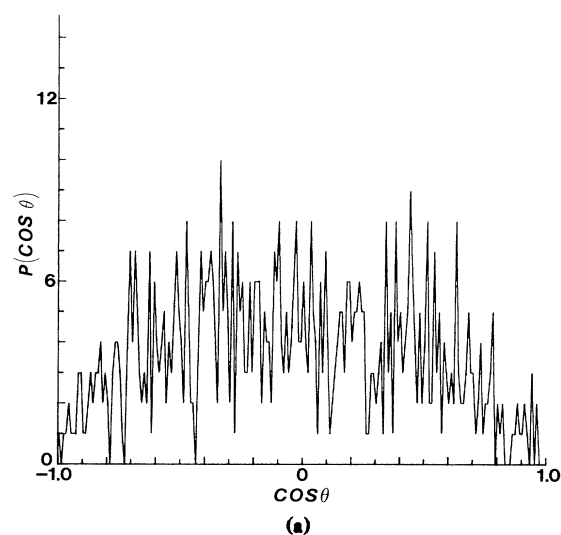
FIG. 3. The probability density for the distribution of the angle between velocity u and vorticity ω conditionally sampled in the region where dissipation is greater than 30% of its maximum value: (a) in the outer part of the channel ($15 < z_+ < 100$); (b) in the Taylor-Green vortex at $t = 8.6$.

FIG. 4. The probability density for the distribution of the angle between velocity u and vorticity ω conditionally sampled in the region where dissipation is less than 5% of its maximum value: (a) in the outer part of the channel ($15 < z_+ < 100$); (b) in the Taylor-Green vortex at $t = 8.6$.

ty are nearly aligned. This result may be useful to understand turbulent flow structures.

A related result of Arnold[12] and Moffatt[13] is that there exist steady, helical Euler flows with arbitrary chaotic, streamline topologies in which u and ω are everywhere parallel: $u = \lambda \omega$ with λ constant. Although the relation between steady, inviscid Euler and time-dependent viscous flows may seem tenuous, the high probability that $|\cos\theta| \approx 1$ in regions of low dissipation maybe suggests that further study of the Arnold-Moffatt flows is warranted.
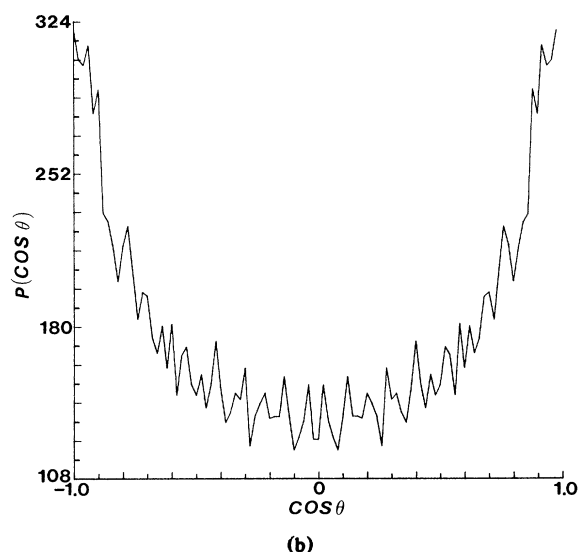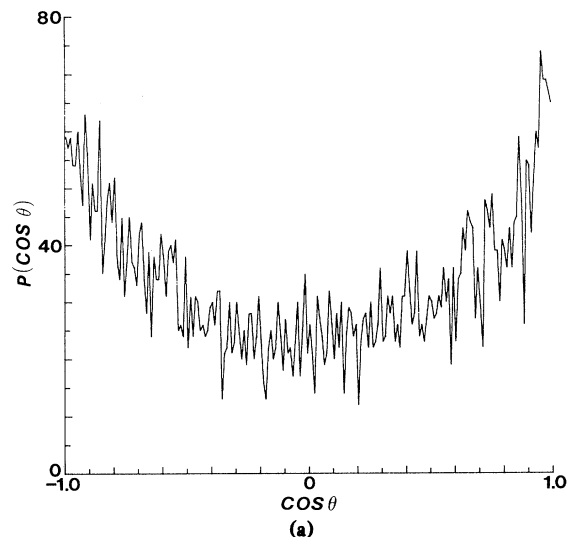
[a]On leave from Tel-Aviv University, Tel Aviv, Israel.

[1]E. Levich and A. Tsinober, Phys. Lett. **93A**, 293–297 (1983).

[2]A. Tsinober and E. Levich, Phys. Lett. **99A**, 321–324 (1983)

[3]E. Levich and A. Tsinober, Phys. Lett. **101A**, 265–272 (1984).

[4]E. Levich and E. Tzvetkov, to be published.

[5]H. K. Moffatt, in *Turbulence and Chaotic Phenomena in Fluids,* edited by T. Tatsumi (North-Holland, Amsterdam, 1984), pp. 223–230.

[6]D. K. Lilly, in *Intense Atmospheric Vortices,* edited by L. Bengtsson and L. Lighthill (Springer, Berlin, 1982).

[7]U. Schhumann, in the Proceedings of the DFVLR Colloquim on Nonlinear Dynamics in Transcritical Flows, Deutsche Forschungs- und Versuchsanstalt fuer Luft- und Raumfahrt, West Germany (Springer, Berlin, to be published).

[8]E. Levich and E. Tzvetkov, Phys. Lett. **100A**, 53–56 (1984).

[9]S. A. Orszag and A. T. Patera, J. Fluid Mech. **128**, 347–385 (1983).

[10]M. E. Brachet, D. I. Meiron, S. A. Orszag, B. G. Nickel, R. H. Morf, and U. Frisch, J. Fluid Mech. **130**, 411–452 (1982).

[11]M. E. Brachet, S. A. Orszag, R. W. Metcalfe, and J. Riley, to be published.

[12]V. I. Arnold, "The Asymptotic Hopf Invariant and its Application," in Proceedings of the Summer School in Differential Equations, Erevan, U.S.S.R. (Armenian SSR Academy of Sciences, Erevan, U.S.S.R., 1974).

[13]H. K. Moffatt, to be published.